CANCER GENOMICS & PROTEOMICS *21*: 591-607 (2024)
doi:10.21873/cgp.20476

Impact of Hypoxia and the Levels of Transcription Factor HIF-1α and JMJD1A on Epithelial-Mesenchymal Transition in Head and Neck Squamous Cell Carcinoma Cell Lines

ARMIN VON FOURNIER, CHRISTIAN WILHELM, CLARA TIRTEY, MANUEL STÖTH, TOTTA EHRET KASEMO, STEPHAN HACKENBERG and AGMAL SCHERZAD

Department of Oto-Rhino-Laryngology, Head and Neck Surgery, University Hospital Wuerzburg, Wuerzburg, Germany

Abstract. *Background/Aim: This study aimed to assess the impact of hypoxia on epithelial-mesenchymal transition (EMT) in head and neck squamous cell carcinoma (HNSCC), focusing on the involvement of transcription factors hypoxia inducible factor 1 (HIF-1α) and Jumonji Domain-Containing Protein 1A (JMJD1A). Materials and Methods: FaDu and Cal33 cell lines were subjected to hypoxic and normoxic conditions. Cell proliferation was quantified electronically, while PCR and western blot analyses were used to measure mRNA and protein levels of HIF-1α, JMJD1A, and EMT markers. EMT was further characterized through immunofluorescence, migration, and invasion assays. Results: Hypoxic conditions significantly reduced cell proliferation after 48 hours in both cell lines. HIF-1α mRNA levels increased initially during short-term hypoxia but declined thereafter, while JMJD1A mRNA levels showed a sustained increase with prolonged hypoxia. Western blot analysis revealed contrasting trends in protein levels. EMT marker expression varied markedly over time at both the mRNA and protein levels, suggesting EMT induction in hypoxia within 24 hours. Immunofluorescence, migration, and invasion assays supported these findings. Conclusion: The study provides evidence of hypoxia-induced EMT in HNSCC, although conflicting results suggest a complex interplay among molecular regulators involved in this process.*

Correspondence to: Armin von Fournier, Josef-Schneider-Strasse 11, D-97080 Wuerzburg, Germany. Tel: +49 93120121476, Fax: +49 93120121321, e-mail: fournier_a@ukw.de

Key Words: Head and neck squamous cell carcinoma, HNSCC, hypoxia, FaDu, Cal33, HIF-1α, JMJD1A, epithelial-mesenchymal transition, EMT.

Hypoxia, characterized by reduced oxygen availability, poses a significant challenge to cellular homeostasis and survival in mammalian cells (1). However, paradoxically, many malignant tumors thrive in environments with heterogeneous oxygen concentrations. Within tumors, hypoxic regions emerge due to inadequate oxygen supply to rapidly proliferating tumor cells (2). This phenomenon is notably observed in head and neck squamous cell carcinomas (HNSCC) (3).

The transcription factor hypoxia-inducible factor (HIF) emerges as a pivotal player in tumor progression and physiological and pathological adaptations to hypoxia (4). Comprising an oxygen-sensitive α subunit and a constitutively expressed β subunit, HIF orchestrates gene expression under hypoxic conditions. There are three known α subunits 1α, 2α and 3α, while the latter is not ubiquitously expressed and is underexplored (5). HIF-1α has a half-life of only a few minutes in normoxia, is stabilized during continuous hypoxia and can accumulate in the nucleus (6). Stable HIF-1α accumulates in the cytosol and translocates to the nucleus where it dimerizes with the constitutively expressed HIF-1β and can bind the hypoxia response element (HRE) of target genes (7).

HIF-1α typically responds within shorter time intervals (2-24 h) and lower oxygen levels (<0.1% O_2) whereas HIF-2α usually reacts in a higher oxygen level (<5% O_2) with a longer maintenance time (48-72 h) in some cell lines (8). In simplified terms, HIF-1α could be seen as a driver of acute hypoxia (<24 h) while HIF-2α is active in the chronic response (>24 h) (9). Primary endothelial cells exhibit a transition from HIF-1α to HIF-2α under conditions shifting from acute to prolonged hypoxia (10). Notably, both subtypes may exhibit tumor-suppressive effects in specific contexts (6, 7, 11).

Elevated HIF expression is observed in primary and metastatic tumors (12, 13). It correlates with tumor hypoxia and is often exacerbated by loss of function of tumor suppressor genes like p53 or von Hippel-Lindau *via* a decreased degradation of HIF-1α. The clonal selection of cancer cells exhibiting heightened HIF-1α activity drives the malignant progression of the tumor (14). Herein, HIF-1α expression has been demonstrated as an early event in oral carcinogenesis (15). Conversely, in the recent literature, there is increasing evidence that hypoxia-independent mechanisms of HIF signaling activation may confer advantageous traits to cancer cells, promoting their survival and development (16). However, it is widely acknowledged that tumor hypoxia significantly hampers the efficacy of tumor therapies, stemming from reduced levels of chemotherapeutics and the intrinsic radiation resistance of hypoxic regions (17). Therefore, HIF presents itself as a promising target for future tumor therapies, given the emergence of novel regulators of HIF-1α in the current literature (18).

HIF activation heralds a cascade of downstream effects, including expression of over a hundred genes influencing angiogenesis, energy metabolism, proliferation, and apoptosis (19-21). JMJD1A, a histone demethylase, emerges as a key mediator of HIF signaling (22, 23). Its oxygen-dependent and HIF-mediated expression has been demonstrated both in vitro and in vivo (24). Its demethylase function regulates the transcription of additional genes, amplifying HIF effects and promoting tumor proliferation and adaptation to the hypoxic microenvironment (25). There are also studies that provide evidence that the HIF-1α/JMJD1A signaling pathway is involved in inflammation and oxidative stress induced by hypoxia, among others (26). Our findings demonstrate that HIF-1α and JMJD1A serve as pertinent hypoxia-dependent regulators of carcinogenesis in HNSCC cell lines (27). JMJD1A regulates cell proliferation in hepatocellular carcinoma under hypoxia through the peptide adrenomedullin, while promoting urinary bladder cancer progression *via* coactivation of HIF-1α (28). Additionally, JMJD1A promotes the proliferation and progression of prostate cancer, emphasizing its potential as a therapeutic target for advanced prostate cancer (29). Under hypoxic conditions, JMJD1A modulates radioresistance in esophageal squamous cell carcinoma cells (30). A recent review underscores the growing importance of histone demethylases such as JMJD1A as prognostic markers and potential therapeutic targets in HNSCC (31).

An integral event in tumor progression activated by hypoxia is epithelial-mesenchymal transition (EMT) (25). In the past, EMT was perceived as a process wherein epithelial tumor cells diminished their epithelial characteristics by downregulating epithelial markers and upregulating mesenchymal ones. This facilitated their migration from the epithelial tumor tissue to distant locations *via* the bloodstream or lymphatic system (32). Recent findings challenge this notion, suggesting that migratory behaviors do not conform to distinct, mutually exclusive categories. Instead, they represent various degrees or combinations of epithelial and mesenchymal features, forming a continuum of morphological diversity among cells and manifesting an array of migratory behaviors (33). This process is also reversible, as elucidated by the concept of mesenchymal-epithelial transition (MET) (34).

Various signaling pathways for hypoxia-induced EMT have been identified, including the transforming growth factor β (TGF-β), wnt-β-catenin, and hedgehog pathways (8). These pathways involve alterations in several EMT transcription factors. Twist stands out as an essential and non-redundant factor in HIF-1α-mediated EMT. Co-expression of Twist with another EMT marker, snail, and HIF-1α correlates with a poor prognosis in HNSCC patients (35). HIF-1α-induced activation of snail has been observed in various tumor entities (36, 37). Additional relevant EMT transcription factors include slug, smad interacting protein 1 (SIP1) and zinc finger E-box binding homeobox 1 (ZEB1). EMT entails the loss or downregulation of epithelial markers such as E-cadherin, alongside the gain or upregulation of mesenchymal markers like N-cadherin and vimentin (38).

Despite the known influence of hypoxia, HIF, and JMJD1A on EMT, particularly in HNSCC, the underlying mechanisms remain elusive. This study aims to elucidate the impact of hypoxia and the roles of HIF-1α and JMJD1A in EMT in HNSCC. Understanding these mechanisms could inform future cancer treatment strategies, enhancing therapeutic efficacy against this challenging disease.

Materials and Methods

Tumor cell incubation. The HNSCC cell lines FaDu and Cal33 were acquired from ATCC (*via* LGC Standards, Wesel, Germany) (39, 40). FaDu cells were cultured in Modified Eagle's Medium (MEM) (Sigma-Aldrich, Schnelldorf, Germany) and Cal33 cells were grown in Dulbecco's Modified Eagle Medium (DMEM) (Gibco Invitrogen, Karlsruhe, Germany). Both media were supplemented with 10% FCS and 1% penicillin/streptomycin (Sigma-Aldrich) and MEM additionally with L-Glutamine (Sigma-Aldrich). Cultures were maintained at 37°C with 5% CO_2, with medium replacement every other day. Upon reaching 70-80% confluence, cells were trypsinized with 0.25% trypsin (Gibco Invitrogen), washed with phosphate-buffered saline (PBS) (Roche Diagnostics GmbH, Mannheim, Germany) and seeded into new culture flasks or treatment wells. Experiments were performed using cells in the exponential growth phase.

Tumor cell proliferation. Tumor cells were initially seeded onto culture plates and incubated for 24 h at 37°C, 19% O_2 and 5% CO_2. Subsequently, five plates (N_1, N_3, N_6, N_{24} and N_{48}) were maintained in normoxic conditions, while another five plates were subjected to hypoxia at 37°C with 5% CO_2 and 1% O_2 (H_1, H_3, H_6, H_{24} and H_{48}) for 1, 3, 6, 24 and 48 h, respectively. Following incubation, the supernatant was aspirated, cells were detached with 0.25% trypsin, DMEM with supplements [10% FCS and 1% penicillin/streptomycin (Sigma-Aldrich)] was added, and cell

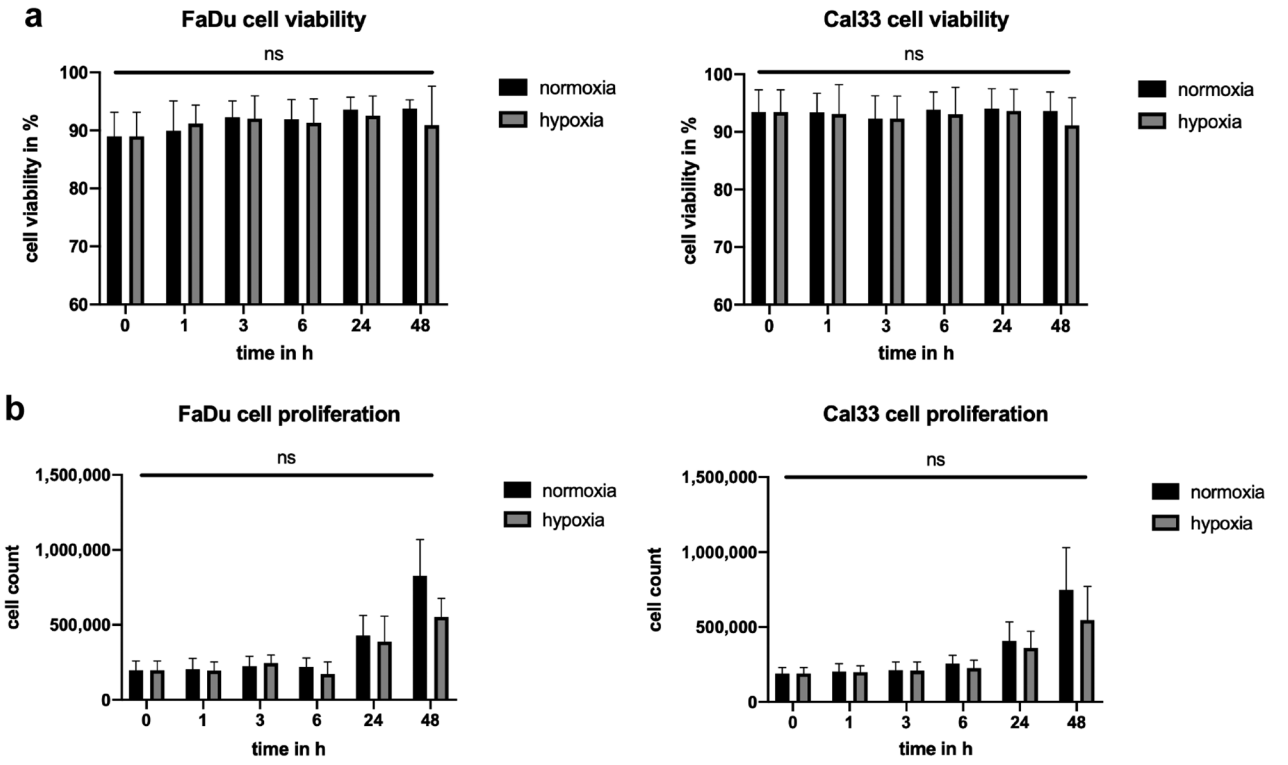

Figure 1. *FaDu and Cal33 cell viability (a) after 0, 1, 3, 6, 24 and 48 h in normoxia and in hypoxia. FaDu and Cal33 cell proliferation (b) after 0, 1, 3, 6, 24 and 48 hours in normoxia and in hypoxia.*

counting was performed electronically (Casy® Technologies, Innovatis AG, Reutlingen, Germany).

Quantitative real-time PCR. Harvesting of tumor cells for Real-time polymerase chain reaction (rt-PCR) was conducted on ice to prevent degradation of *HIF-1α* mRNA. After removing the supernatant, 5ml PBS was added and cells were scraped, resuspended, and centrifuged for 5 min at 4˚C and 1500 rpm. RNA extraction was performed using the RNeasy Mini Kit (Qiagen, Hilden, Germany) following the manufacturer's protocol. RNA concentration was determined spectrophotometrically (Eppendorf AG, Hamburg, Germany). cDNA synthesis was carried out using 50 ng of RNA using SuperScript VILO Mastermix (Thermo Fisher Scientific, Waltham, MA, USA) at 42˚C. Two microliters of template cDNA were added to a final volume of 20 µl of reaction mixture consisting of 10 µl TaqMan Gene Expression Master Mix, 1 µl of the corresponding TaqMan Gene Expression Assays (assay IDs: *HIF-1α*=Hs00153153_m1, *HIF-2*=Hs01026149_m1, *KDM3A/JMJD1A*=Hs00218331_m1, *E-Cadherin*=Hs01023895_m1, *Occludin*=Hs00170162_m1, *Snail*=Hs00195591_m1, *Twist*=Hs01675818_m1, *Vimentin*=Hs00958111_m1, all from Thermo Fisher Scientific) and 7 µl RNAse free water. PCR cycle parameters included an initial step at 50˚C for 2 min, enzymatic activation for 10 min at 95˚C, followed by 40 cycles involving denaturation at 95˚C for 15 s, followed by the annealing and the extension of the primer, and subsequently amplification at 60˚C for 1 min. Relative gene expression levels of *HIF-1α* and *KDM3A/JMJD1A* were quantified using fluorescent TaqMan® technology. GAPDH (Hs02758991_g1, Thermo Fisher Scientific) served as an endogenous control. Additionally, each sample was measured in triplicate and the comparative Ct method was employed for relative quantification of gene expression as described previously (41). Data were expressed as the mean of three independent experiments.

Western blot. For western blot analysis, cell harvesting was performed on ice to prevent degradation of HIF-1α protein. Following removal of the supernatant, the lysis buffer [comprised of 25% NuPAGE™ LDS sample buffer (Thermo Fisher Scientific) and 3% 2-mercaptoethanol] was added for homogenization. Cell lysates were then heated at 70˚C for 10 min and subsequently centrifuged after cooling. Supernatants were utilized for western blot analysis, where 20 µl of the lysate was electrophoresed and transferred to a nitrocellulose membrane. After washing in distilled water for 5 min, membranes were blocked for 60 min with blocking buffer [5% non-fat dry milk, TBST (10 mM Tris-HCl pH 8.0, 150 mM NaCl, 0.1% Tween 20)]. Subsequently, membranes were washed in TBST three times for 5 min and incubated with primary antibodies (pAb) at 7˚C overnight, with the following dilutions: anti-E-Cadherin 1:500 (Cat. No. Sc-21791, Santa Cruz Biotechnology, Dallas, TX, USA), anti-HIF-1α 1:1000 (Cat. No. MA1-516, Thermo Fisher Scientific), anti-HIF-2 1:1000 (Cat. No. PA1-16510, Thermo Fisher Scientific), anti-JMJD1A 1:1000 (Cat. No. PA5-88279, Thermo Fisher Scientific), anti-Occludin 1:1000 (Cat. No. 40-4700, Thermo Fisher Scientific), anti-Snail 1:1000 (Cat. No. C15D3, Cell Signaling Technology, Danvers, MA, USA), anti-Twist 1:1000, (Cat. No. MA5-38652, Thermo Fisher Scientific) and anti-Vimentin 1:1000 (Cat. No. D21H3, Cell Signaling Technology). After three washes with TBST, membranes were

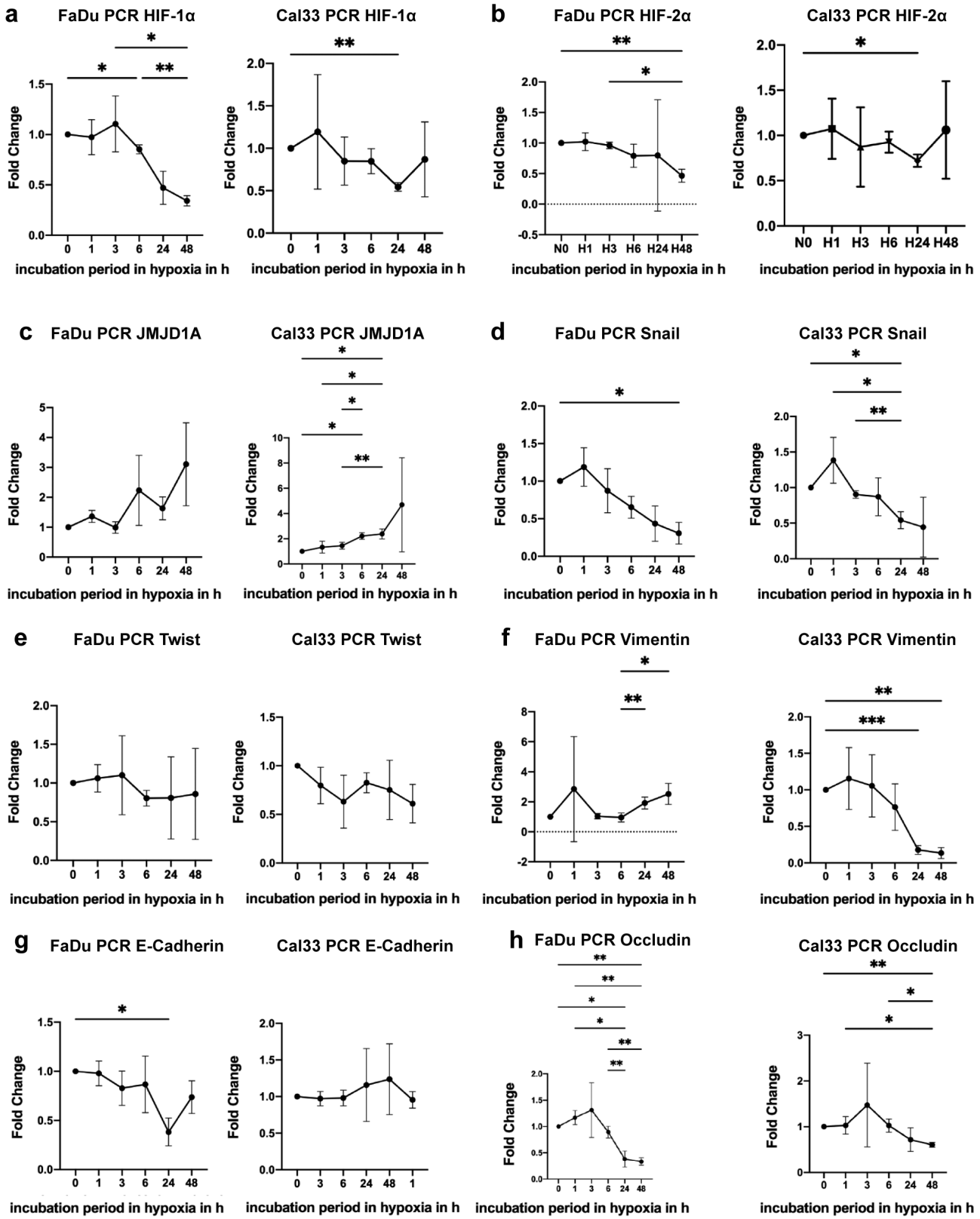

Figure 2. *mRNA levels in the quantitative real-time PCR in FaDu and Cal33 cells. HIF-1α mRNA (a), HIF-2α mRNA (b), JMJD1A mRNA (c), Snail mRNA (d), Twist mRNA (e), Vimentin mRNA (f), E-Cadherin mRNA (g), Occludin mRNA (h).*

incubated for 1 h with horse radish peroxidase-conjugated anti-mouse (Cat. No. A9044, Sigma-Aldrich) or anti-rabbit (Cat. No. 111-035-003, Jackson ImmunoResearch, West Grove, PA, USA) IgG at a dilution of 1:10000. Finally, the signals were developed using the SuperSignal West Atto Maximum Sensitivity Substrate Enhanced Chemiluminescence (Thermo Fisher Scientific) and transferred to the iBright™ CL1500 Imaging System (Thermo Fisher Scientific). Protein expression levels were quantified using the iBright™ Analysis Software (Thermo Fisher Scientific).

Immunofluorescence. Tumor cells were seeded onto microscopic slides and cultured on plates, similarly to the proliferation experiments. Following incubation, the medium was removed, and cells were fixed in a fixation solution [4% paraformaldehyde (Carl Roth, Karlsruhe, Germany) in PBS] for 30 min, followed by two washes in PBS. Subsequently, cells were incubated in 1% Triton X-100 (Merck, Darmstadt, Germany) for 15 min and in a blocking solution [0.1% Tween, 0.5% Triton X-100, 1% Albumin Fraction V (Carl Roth) and 10% normal horse serum (NHS, Gibco Invitrogen) in PBS] for one hour. Cells were then incubated with pAb at 4˚C overnight, with the following dilutions: anti-E-Cadherin 1:100 (Cat. No. Sc-21791, Santa Cruz Biotechnology), anti-HIF-1α 1:100 (Cat. No. MA1-516, Thermo Fisher Scientific), anti-HIF-2 1:150 (Cat. No. PA1-16510, Thermo Fisher Scientific), anti-JMJD1A 1:100 (Cat. No. PA5-88279, Thermo Fisher Scientific), anti-Occludin 1:1,000 (Cat. No. 40-4700, Thermo Fisher Scientific), anti-Snail 1:100 (Cat. No. 14-9859-82, Thermo Fisher Scientific), anti-Twist 1:500, (Cat. No. MA5-38652, Thermo Fisher Scientific) and anti-Vimentin 1:100 (Cat. No. D21H3, Cell Signaling Technology). After three washes with PBS, cells were incubated for 1 h with horse radish peroxidase-conjugated anti-mouse (Cat. No. A32766, Invitrogen) or anti-rabbit (Cat. No. A32794, Invitrogen) IgG at a dilution of 1:1000. Following three additional washes with PBS, cells were incubated with 0.03% 4',6-diamidino-2-phenylindole (DAPI) (Cat. No. D9542, Merck) in PBS. After two washes in PBS, cells were fixed with Aqua-Poly/Mount (Polysciences, Warrington, PA, USA). Visualization of cells was performed under the Leica DMi8 Microscope (Leica, Wetzlar, Germany) at 20× magnification with fixed exposure times. Morphological cell analysis without immunostaining was conducted using the Leica DMI4000 B Microscope (Leica) at 10× and 40× magnification.

Scratch and invasion assay. For the scratch assay, cells were seeded in culture plates and allowed to reach 70-80% confluence. A gap was then created in the middle of the plate by scratching with a pipette tip. Following this, the medium was changed, and any loose cells were removed. Imaging was conducted using the Leica DMI4000 B Microscope at 4× magnification immediately after scratching and again after 24 and 48 h in both normoxia and hypoxia conditions. Image analysis was performed using ImageJ 1.53a Software (National Institute of Health, Bethesda, MD, USA).

For the invasion assay, Matrigel™ Matrix Basement Membrane (Ref No 354230) (Corning, Corning, NY, USA) was applied to 8 μm pore Transwell™ plates (Greiner Bio One, Frickenhausen, Germany) and incubated at 37˚C for 30 min. The lower chamber of the well was filled with FCS-free medium, and cells were seeded in the transwell in FCS-free medium and incubated for 24 h. Subsequently, the medium was changed, and cells were further incubated for 24 and 48 h in normoxia and hypoxia, respectively. After incubation, the Matrigel™ Matrix was removed, and the cells were stained for 20 min in 1% crystal violet solution (K. Hollborn & Söhne, Leipzig, Germany). The plates were then washed with distilled water and 10% acetic acid. To remove any loose, stained cells, the supernatant was centrifuged for one min. The intensity of the staining, indicative of the number of invaded cells, was quantified by measuring the absorbance in the microplate reader Bio ELx800 (BioTek Instruments, Friedrichshall, Germany).

Statistical analysis. All data were compiled into standard spreadsheets and subjected to statistical analysis (GraphPad Prism 9.3.1 Software, La Jolla, CA, USA). Given the assessment of multiple factors in the proliferation experiments (various oxygenation levels across different incubation periods), a 2-way ANOVA was employed to assess statistical significance. To account for multiple comparisons, Šidák's multiple comparison test was applied.

For the statistical analysis of PCR and western blot data, a one-way ANOVA was utilized since the comparison was made across different hypoxia incubation periods rather than against normoxic conditions. To address potential lack of sphericity, a Geisser-Greenhouse correction was applied. Tukey's multiple comparison test was then conducted for correction of multiple testing.

Correlations between different targets in PCR and Western Blot analyses were examined using Spearman's rank-order correlation. In contrast, paired *t*-tests were performed to analyze the scratch and invasion assays. Statistical significance was considered at $p<0.05$, with asterisks indicating significant differences.

Results

Tumor cell viability and proliferation. The viability of FaDu and Cal33 was stable between 88 and 95% in normoxia and hypoxia until 48 h, without any significant differences between these two conditions (Figure 1a). FaDu cell proliferation was low in the first h both in normoxia and hypoxia. After 24 h, proliferation increased more intensely in normoxia (262±37%) than in hypoxia (228±46%). After 48 h, differences in proliferation increased to 552±66% in normoxia and 363±34% in hypoxia. Differences were not statistically significant ($p=0.30$ for different levels of oxygenation).

Cal33 cell proliferation was similar to FaDu. After 24 h, proliferation increased to 272±85% in normoxia and 241±74% in hypoxia. After 48 h, the proliferation benefit in normoxia increased to 499±38% compared to 364±41% in hypoxia. Differences were not statistically significant ($p=0.38$ for different levels of oxygenation, Figure 1b).

Real-time PCR, western blot and immunofluorescence. Statistical analysis found several significant correlations between the studied genes and proteins in PCR and Western Blot. Immunofluorescence staining was performed for the same periods of hypoxia as in PCR and Western Blot. The results in normoxia and after 24 and 48 h of hypoxia are shown.

HIF-1α. For FaDu cells in hypoxia, *HIF-1α* mRNA levels increased after 1 and 3 h (H_3:111±28%), then decreased below the baseline after 6 h (H_6:85±4%) and further after 48 h (H_{48}:34±5%). Differences were statistically significant ($p=0.002$ between 6 and 48 h). For Cal33 cells in hypoxia,

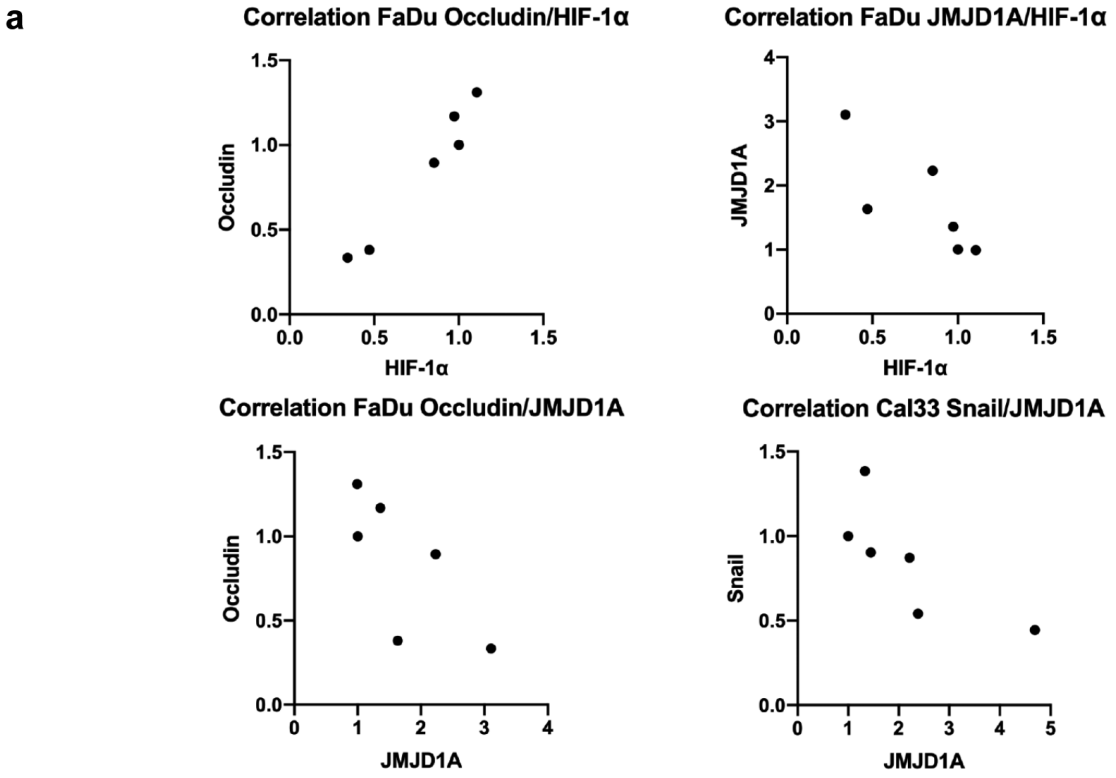

Figure 3. *Continued*

HIF-1α mRNA levels also initially increased after 1 h (H_1:120±68%), and then continuously decreased to about the half of the baseline after 24 h (H_{24}:54±5%). After 48 h levels increased again (H_{48}:87±44%). Differences were statistically significant (p=0.002 between 0 and 24 h, Figure 2a). Concerning the PCR in FaDu, HIF-1α mRNA showed a direct correlation with occludin mRNA (p=0.008), and an indirect correlation with JMJD1A mRNA (p=0.008) (Figure 3a).

In the Western blot, for FaDu in hypoxia, HIF-1α protein showed a continuous decrease up to 6 h (H_6:60±21%) and increased again up to 48 h (H_{48}:105±66%). Differences were not statistically significant. For Cal33 in hypoxia, HIF-1α protein continuously increased after 48 h (H_{48}:204±68%). Differences were statistically significant (p=0.009 between 1 and 48 h, Figure 4a). In Cal33, HIF-1α protein showed a direct correlation with twist protein (p=0.001) and E-cadherin protein (p=0.008) and an indirect correlation with vimentin protein (p=0.008) and JMJD1A protein (p=0.029) (Figure 3b).

Concerning immunofluorescence in FaDu cells, there was nearly no signal for HIF-1α in normoxia while there was a strong signal in the cytosol after 24 h in hypoxia which further increased after 48 h in hypoxia. In Cal33, the signal for HIF-1α increased after 24 h in hypoxia. After 48 h in hypoxia the low number of surviving cells showed an even stronger signal (Figure 5).

JMJD1A. Concerning FaDu cells in hypoxia, differences in *JMJD1A* mRNA levels were not statistically significant. For Cal33 cells in hypoxia, *JMJD1A* mRNA levels continuously increased after 6 h (H_6:221±26%) and reached a maximum after 48 h (H_{48}:469±373%). Differences were statistically significant up to 24 h (p=0.028 between 0 and 24 h, Figure 2c). JMJD1A mRNA in FaDu correlated indirectly with occludin mRNA (p=0.017). In Cal33, JMJD1A mRNA showed an indirect correlation with snail (p=0.008) and vimentin mRNA (p=0.029, Figure 3a).

In the Western blot for FaDu cells in hypoxia, JMJD1A protein showed a slight increase up to 6 h (H_6:111±58%), followed by a decrease after 24 h (H_{24}:50±15%) and another increase after 48 h (H_{48}:80±27%). Differences were statistically significant up to 24 h (p=0.031 between 0 and 24 h). For Cal33 in hypoxia, JMJD1A protein showed a strong decrease in the first h (H_1:72±16%), followed by stable levels up to 6 h and another decrease up to 48 h (H_{48}:29±12%). Differences were statistically significant (p=0.006 between 0 and 48 h, Figure 4c). In FaDu cells, JMJD1A protein levels correlated indirectly with twist protein levels (p=0.029). In Cal33, JMJD1A protein correlated indirectly with Twist (p=0.029) and E-cadherin protein (p=0.008, Figure 3b).

In immunofluorescence, the JMJD1A signal was slightly stronger after 24 h of hypoxia while it was similarly weak both in normoxia and hypoxia after 48 h. Some cell nuclei

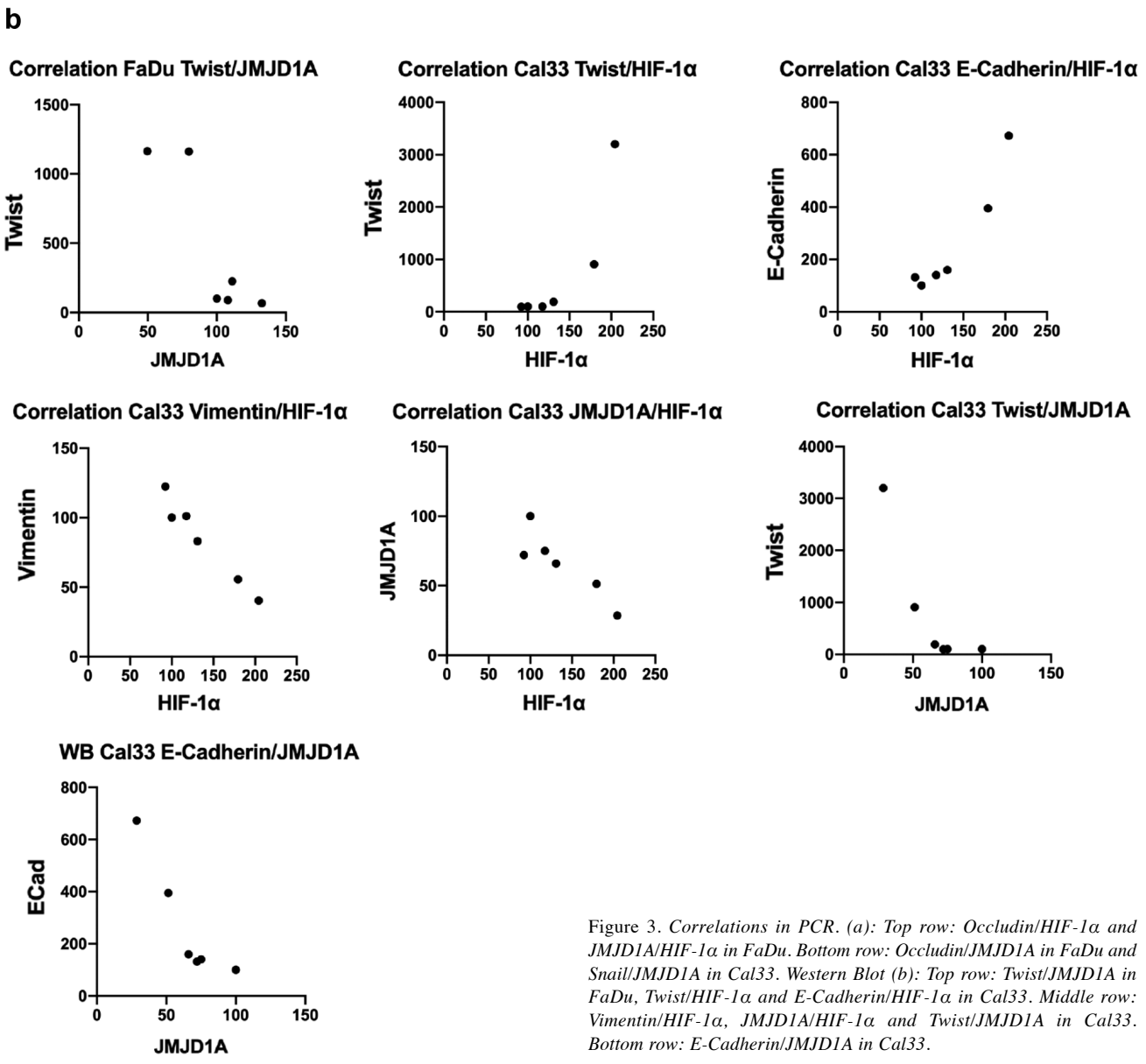

Figure 3. *Correlations in PCR. (a): Top row: Occludin/HIF-1α and JMJD1A/HIF-1α in FaDu. Bottom row: Occludin/JMJD1A in FaDu and Snail/JMJD1A in Cal33. Western Blot (b): Top row: Twist/JMJD1A in FaDu, Twist/HIF-1α and E-Cadherin/HIF-1α in Cal33. Middle row: Vimentin/HIF-1α, JMJD1A/HIF-1α and Twist/JMJD1A in Cal33. Bottom row: E-Cadherin/JMJD1A in Cal33.*

appeared more prominently stained in normoxia (Figure 6a). In Cal33, JMJD1A signal was strong in hypoxia and normoxia with a focus on the nuclei. The overlay with DAPI shows a slightly lower signal of JMJD1A in both incubation periods of hypoxia (Figure 6b).

HIF-2α, Snail, Twist, Vimentin, E-cadherin, Occludin. The change in mRNA levels in the quantitative real-time PCR in FaDu and Cal33 cells can be seen in Figure 2b and d-h and in the protein levels in the Western Blot in Figure 4b and d-h. Immunofluorescence staining for Snail and Occludin in FaDu cells. The corresponding immunofluorescence staining is shown in Figure 5, Figure 6, Figure 7, and Figure 8.

Migration and invasion assay. Migration assay. For FaDu, the area of the scratch decreased to half of the baseline after 24 h in normoxia (N_{24}=49±17%) and was stable after 48 h in normoxia (N_{48}=52±8%). The difference between the baseline and 48 h in normoxia was statistically significant (p=0.008). The area of the scratch was stable after 24 h in hypoxia (H_{24}=90±19%) and decreased similarly to the same time in normoxia after 48 h in hypoxia (H_{48}=56±24%) while the difference to the baseline was not statistically significant. There were no statistically significant differences between normoxia and hypoxia (Figure 9a).

For Cal33, the area of the scratch decreased to about two thirds of the baseline after 24 h in normoxia (N_{24}=66±7%)

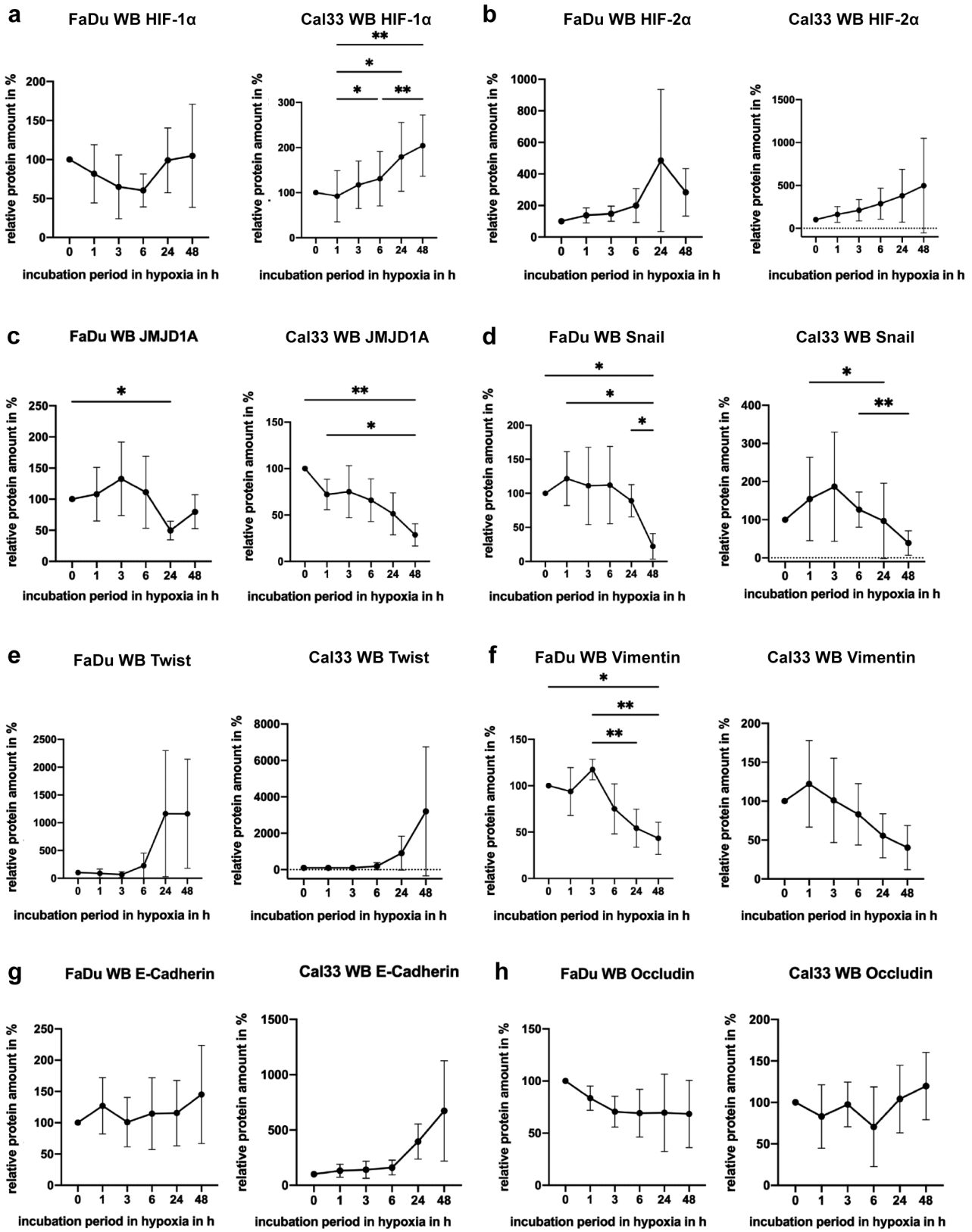

Figure 4. *Protein levels in the Western Blot in FaDu and Cal33 cells. HIF-1α protein (a), HIF-2α protein (b), JMJD1A protein (c), Snail protein (d), Twist protein (e), Vimentin protein (f), E-Cadherin protein (g), Occludin protein (h).*

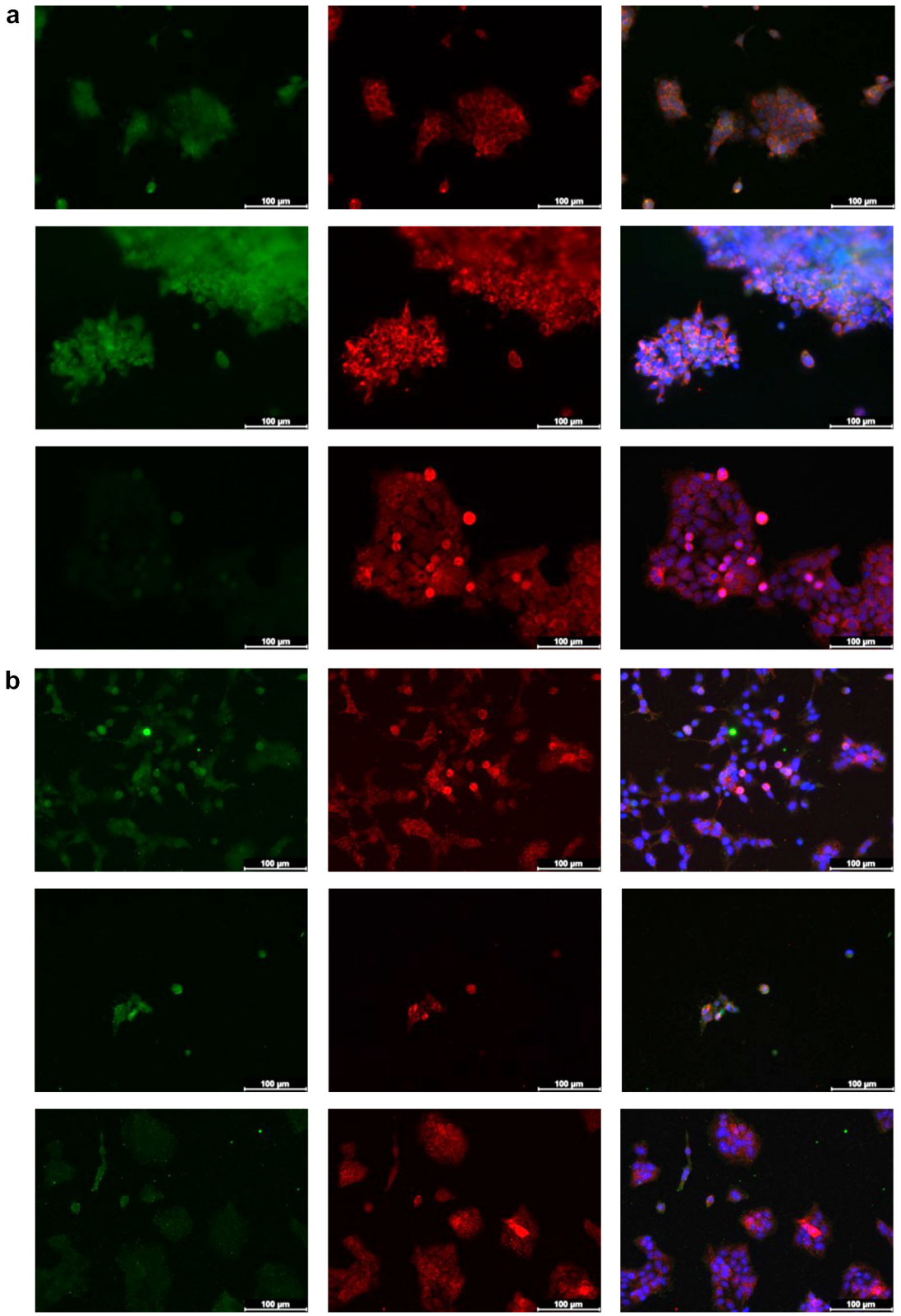

Figure 5. *(a) Immunofluorescence staining for HIF-1α and HIF-2α in FaDu cells. From left to right HIF-1α, HIF-2α and overlay. Top row corresponds to 24 h hypoxia, middle row to 48 h hypoxia, bottom row to normoxia. (b) Immunofluorescence staining for HIF-1α and HIF-2α in Cal33 cells. From left to right HIF-1α, HIF-2α and overlay. Top row corresponds to 24h hypoxia, middle row to 48 h hypoxia, bottom row to normoxia.*

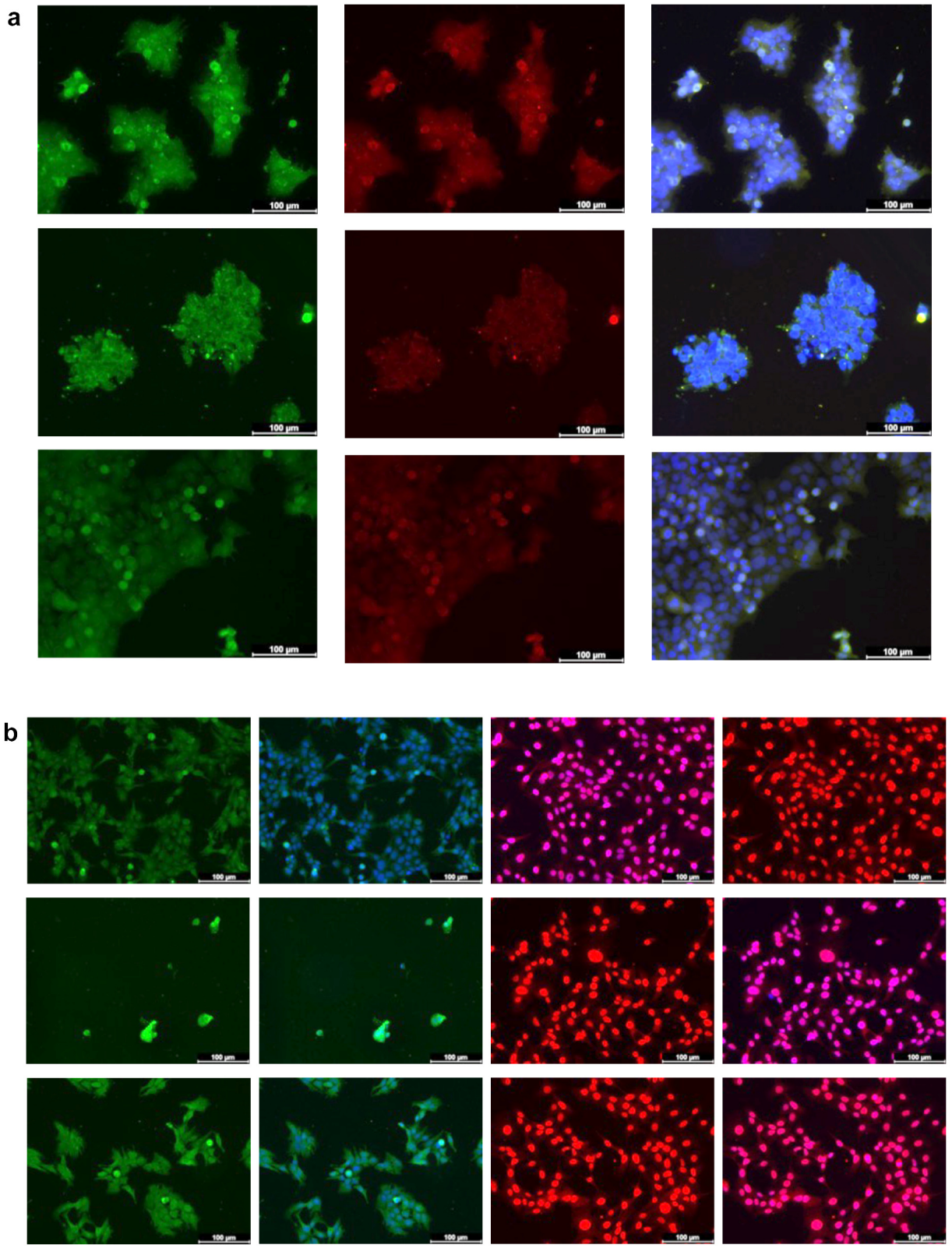

Figure 6. *(a) Immunofluorescence staining for Twist and JMJD1A in FaDu cells. From left to right Twist, JMJD1A and overlay. Top row corresponds to 24 h hypoxia, middle row to 48 h hypoxia, bottom row to normoxia. (b) Immunofluorescence staining for Twist and JMJD1A in Cal33 cells. From left to right Twist, overlay, JMJD1A and overlay. Top row corresponds to 24 h hypoxia, middle row to 48 h hypoxia, bottom row to normoxia.*

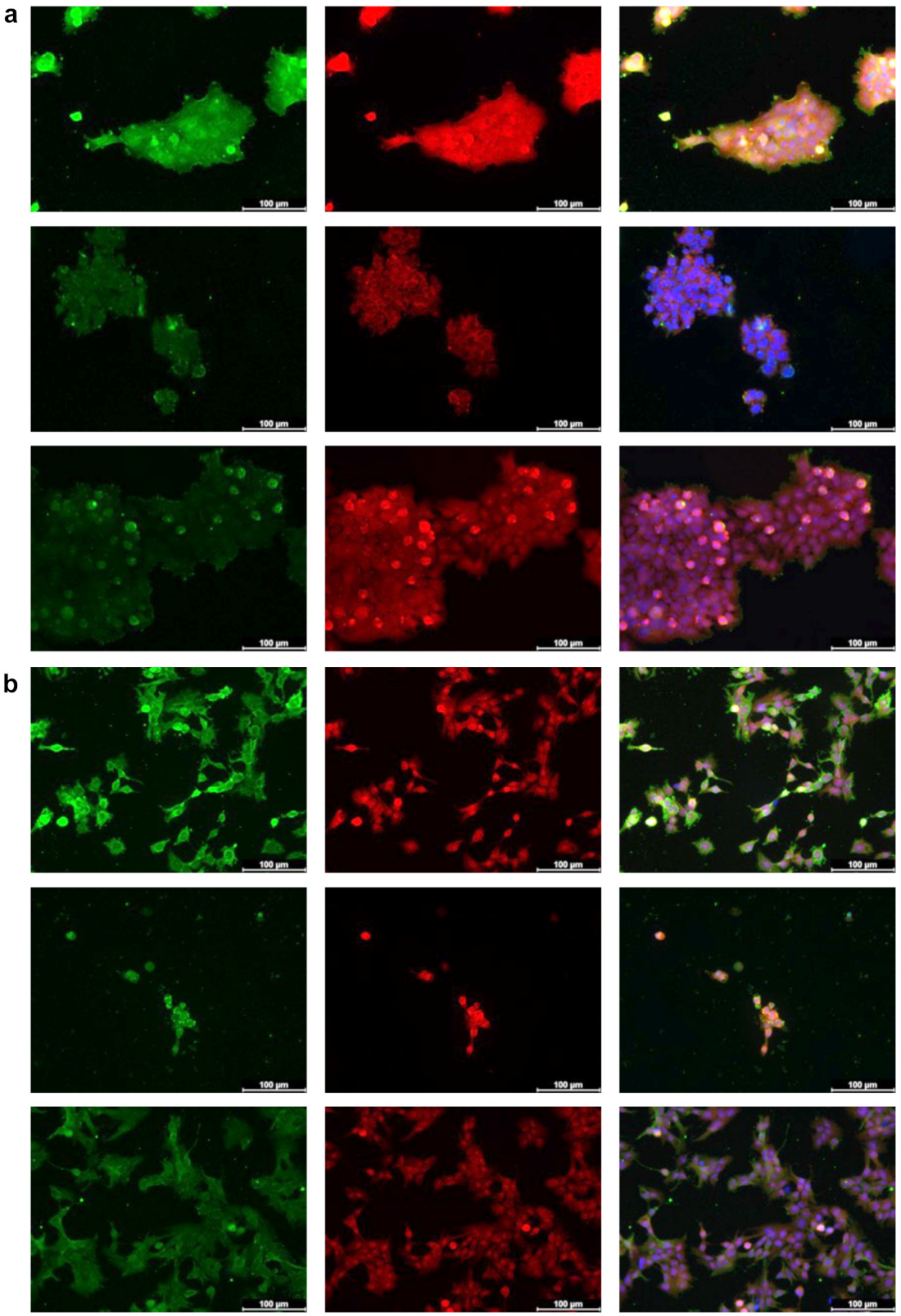

Figure 7. *(a) Immunofluorescence staining for Snail and Occludin in FaDu cells. From left to right Snail, Occludin and overlay. Top row 24h hypoxia, middle row 48 h hypoxia, bottom row normoxia. (b) Immunofluorescence staining for Snail and Occludin in Cal33 cells. From left to right Snail, Occludin and overlay. Top row 24 h hypoxia, middle row 48 h hypoxia, bottom row normoxia.*

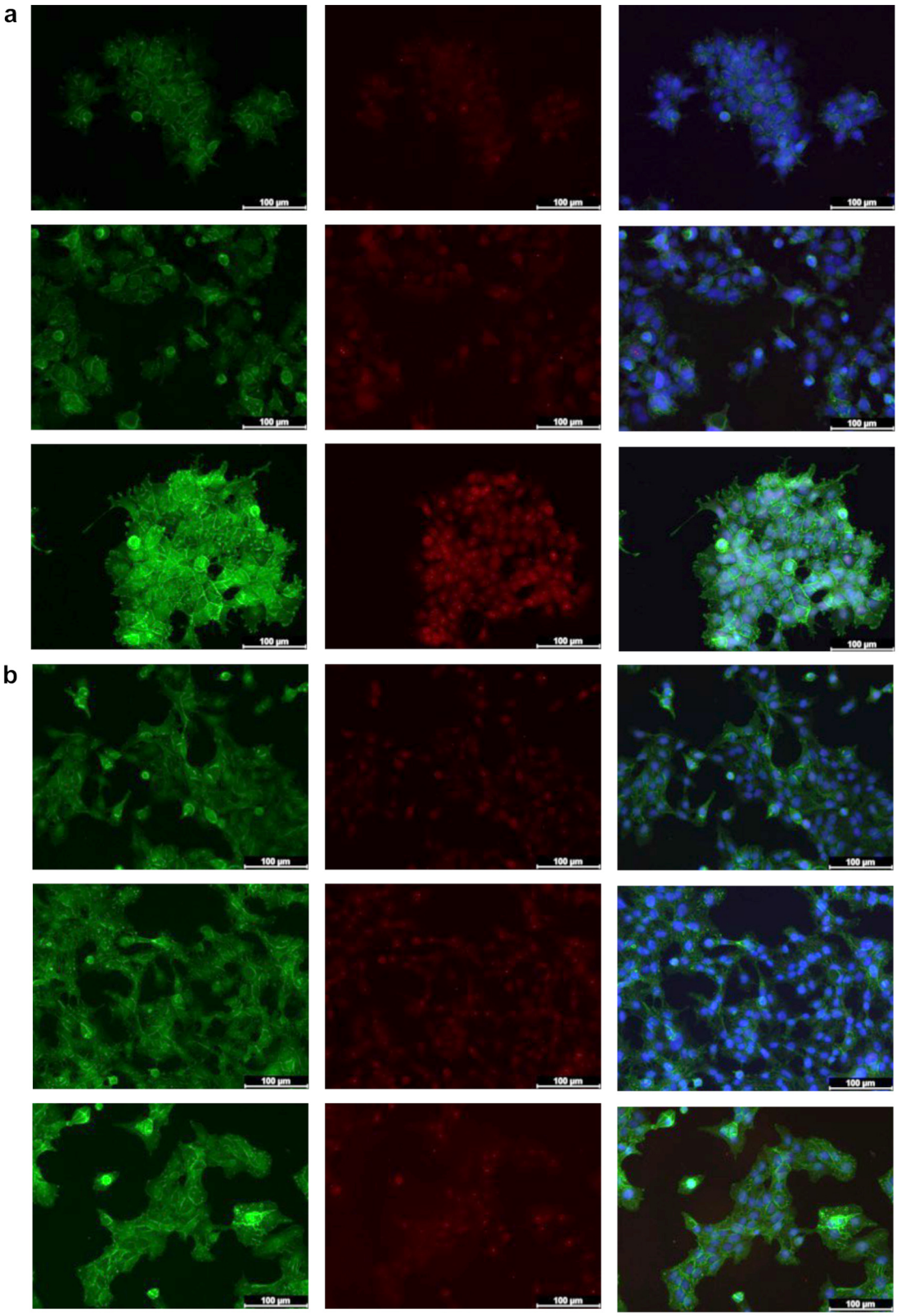

Figure 8. *(a) Immunofluorescence staining for E-Cadherin and Vimentin in FaDu cells. From left to right E-Cadherin, Vimentin and overlay. Top row 24 h hypoxia, middle row 48 h hypoxia, bottom row normoxia. (b) Immunofluorescence staining for E-Cadherin and Vimentin in Cal33 cells. From left to right E-Cadherin, Vimentin and overlay. Top row 24 h hypoxia, middle row 48 h hypoxia, bottom row normoxia.*

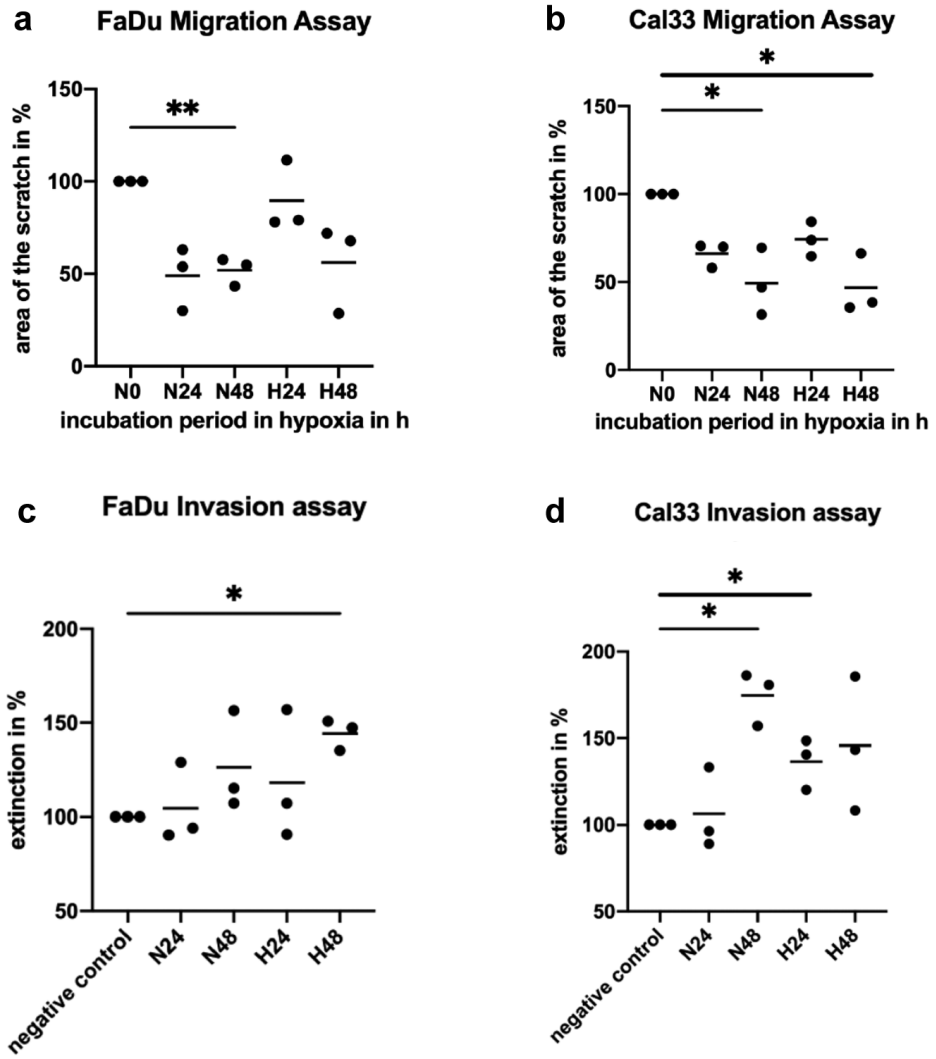

Figure 9. *Migration and invasion assays. Migration assay in FaDu cells (a) and in Cal33 cells (b). Invasion assay in FaDu cells (c) and in Cal33 cells (d).*

and further decreased to nearly half of the baseline after 48 h in normoxia (N_{48}=49±19%). The difference between the baseline and 48 h in normoxia was statistically significant (p=0.045). The area of the scratch decreased to a slightly lesser extent after 24 h in hypoxia (H_{24}=74±10%) and then decreased more after 48 h in hypoxia (H_{48}=47±17%) when compared to normoxia. The difference between the baseline and 48 h in normoxia was statistically significant (p=0.032). There were no statistically significant differences between normoxia and hypoxia (Figure 9b).

Invasion assay. For FaDu, the differences after 24 h in normoxia (N_{24}=105±21%) compared to the baseline and after 48 h in normoxia (N_{48}=126±26%) were not statistically significant. The extinction slightly increased after 24 h in hypoxia (H_{24}=118±35%) and increased more strongly after 48 h in hypoxia compared to normoxia (H_{48}=145±8%). The difference between the baseline and 48 h in hypoxia was statistically significant (p=0.011). There were no statistically significant differences between normoxia and hypoxia (Figure 9c).

For Cal33, the extinction was again stable after 24 h in normoxia (N_{24}=106±24%). After 48 h in normoxia, the extinction increased to nearly twofold (N_{48}=175±16%). The difference between the baseline and 48 h in normoxia was statistically significant (p=0.014). The extinction increased more clearly after 24 h in hypoxia when compared to normoxia (H_{24}=137±15%) and then was mainly stable after 48 h in hypoxia (H_{48}=146±39%). The difference between the baseline and 24 h in hypoxia was statistically significant (p=0.049). There were no statistically significant differences between normoxia and hypoxia (Figure 9d).

Discussion

In our study, we investigated the impact of hypoxia and the roles of the transcription factors *HIF-1α* and *JMJD1A* on EMT in two HNSCC cell lines. We observed that the viability of FaDu and Cal33 cells remained stable around 90% under both hypoxic and normoxic conditions. However, proliferation was notably reduced after 48 hours of hypoxia compared to normoxia, consistent with previous findings of our group with FaDu and HLaC78 cells (23).

Analysis of *HIF-1α* mRNA levels revealed slight increases after 1 and 3 h of hypoxia, followed by a continuous decrease up to 48 hours in FaDu cells, consistent with previous findings with FaDu and HLaC78 cells (23). Cal33 cells showed similar trends up to 24 h but continued to exhibit increased levels up to 48 h. *JMJD1A* mRNA levels increased to more than threefold in hypoxia in both FaDu and Cal33 while there was a singular decrease after 24 h in FaDu. FaDu and HLaC78 had shown similarly distinct increases in our previous work (27). Furthermore, other works also showed an accumulation of HIF-1α in FaDu cells already after just 1 h of hypoxia (42). In renal cell carcinoma, JMJD1A mRNA was increased in a hypoxic environment (43).

Western blot analysis demonstrated increased HIF-1α protein levels in hypoxic FaDu and Cal33 cells, with a temporary decrease observed after 6 h in FaDu cells. Previously, we have shown contradictory results in FaDu and HLaC78 cells with a maximum of HIF-1α protein after 6 h and a subsequent decrease (27). JMJD1A protein levels showed inconsistent patterns in hypoxia with an undulatory course in FaDu and a mix of decrease and stable levels in Cal33. In contrast, our previous results showed stable levels in HLaC78 and an increase after prolonged hypoxia in FaDu (23). In synopsis, the effects of hypoxia on JMJD1A mRNA and protein clearly differ within different HNSCC cell lines. Interestingly, Park *et al*. found an upregulation of JMJD1A mRNA and protein under 24 h of hypoxia in the two different hepatoma cell lines HepG2 and Hep3B, whereas no changes were observed in the breast cancer cell line MDA-MB-231 (44). The authors conclude that JMJD1A might be a key regulatory factor for hypoxia-induced cell proliferation in hepatoma, but not in the aforementioned breast cancer cell line. Our results suggest a similarly differing impact of JMJD1A in HNSCC cell lines, indicating variability in their response to hypoxia.

Evaluation of EMT markers through PCR, western blot, and immunofluorescence staining revealed a broad range of expression patterns. Within the first 24 hours of hypoxia, both cell lines exhibited indications of EMT, characterized by increased expression of mesenchymal markers (vimentin, snail, twist) and decreased expression of epithelial markers (E-cadherin in FaDu cells. Cal33 exhibited comparable trends, albeit with E-cadherin mRNA levels remaining constant. Occludin increased in both FaDu and Cal33, which does not support the previous findings. After longer periods of hypoxia up to 48 h, the changes of EMT markers were inconclusive in FaDu and even contradicted a possible EMT in Cal33.

Within 24 h, western blot analysis hinted at an EMT in Cal33 cells, evidenced by increased snail and vimentin levels alongside decreased occludin expression. Twist and E-cadherin remained relatively stable. However, after 48 hours of hypoxia, these trends reversed. In FaDu, western blot analysis was inconclusive within the first 24 h and, like in Cal33, also contradicted EMT after 48 h.

To pinpoint the observed EMT marker alterations within cells, we performed immunofluorescence staining corresponding to the respective incubation periods under hypoxic conditions. In FaDu, the changes of twist, snail, occludin and E-cadherin within 24 h of hypoxia suited a possible EMT. The changes of vimentin, however, were inconclusive. In Cal33, snail, occludin and E-cadherin supported EMT, but twist and vimentin showed contradicting results.

Functional assays including migration and invasion assays supported the presence of EMT features, albeit with differing timelines between the two cell lines. The migration assay revealed an increased migration and thus a tendency for an EMT in FaDu cells only after more than 24 h in hypoxia. The results of Cal33, however, suggested an EMT within 24 h in hypoxia, whereas migration was reduced after 48 h. The invasion assay suggested changes apposite to an EMT only after longer incubation of 48 h in hypoxia.

Overall, our findings suggest that hypoxia induces EMT in FaDu and Cal33 cells within the first 24 hours, with opposing effects observed after prolonged hypoxia. These results align with previous literature indicating a role for hypoxia in promoting EMT in HNSCC. Essid *et al*. found that in Cal33 spheroids, a combination of hypoxia and growth factors was essential to induce EMT (45). Hypoxia-induced EMT has been documented in the HNSCC cell line Tu686. Moreover, hypoxia was found to enhance Tu686 migration and invasion, with the oncogene metadherin implicated in facilitating these processes (46). In nasopharynx carcinoma, hypoxia promoted EMT, and this effect could be reversed by a specific microRNA (47).

The role of HIF-2α for EMT and metastasis in HNSCC is still unclear. As mentioned before, HIF-1α could be seen as a driver of acute hypoxia up to 24 h while HIF-2α is active in a chronic response. In pancreatic cancer, HIF-2α promotes EMT by regulating Twist2 binding to the promoter of E-cadherin, making HIF-2α and this pathway a possible therapeutic target for pancreatic cancer (48). We found stable or decreasing levels of *HIF-2α* mRNA in both FaDu and Cal33 and only a slight increase after 48 h in Cal33. In FaDu, HIF-2α protein strongly increased up to 24 h in hypoxia and decreased afterwards. In Cal33, HIF-2α protein steadily increased up to 48 h in hypoxia. In summary, there

are hints for an upregulation of HIF-2α in prolonged hypoxia in Cal33, but contradictory results in FaDu. Taking into account that the activation of *JMJD1A,* for example, is specific for HIF-1α while it is not activated by isoforms like HIF-2α, there might be a similarly distinct impact of HIF-1α and HIF-2α for EMT (49).

The precise mechanisms linking hypoxia and EMT in HNSCC remain elusive. However, the induction of EMT by hypoxia-inducible factor (HIF) through oncogenic pathways has emerged as a pivotal determinant for metastasis in oral squamous cell carcinoma (34). In prostate cancer, a potential mechanism through which hypoxia and HIF regulate EMT has been elucidated, involving the FoxM1 pathway (50). In the colorectal cancer cell line LoVo, growth differentiation factor 15 has been identified as a promoter of cell viability, invasion, and migration by inducing EMT (51). Several signaling pathways are currently under investigation. For instance, in an intestinal epithelial cell line, the constitutive activation of the MAP kinase MEK1 has been linked to the induction of EMT. This transition is associated with tumor invasion and metastasis *in vivo*, likely mediated by the upregulation of oncogenic factors (52). As previously noted, the transcription factor of interest, JMJD1A, has been demonstrated to facilitate the proliferation and advancement of prostate cancer cells by enabling Snail transcriptional activation. This underscores JMJD1A's potential as a therapeutic target for advanced prostate cancer (29). The literature on the molecular mechanisms of EMT in HNSCC remains relatively sparse. However, a noteworthy study discovered that silencing snail, a key regulator of EMT, can reverse the process and enhance radiosensitivity in hypopharyngeal carcinoma (53).

Conclusion

In summary, hypoxic conditions lasting up to 24 h in two HNSCC cell lines appear to induce EMT, as evidenced by molecular-level changes and functional analyses. However, contradictory results within different tumor cells suggest a complex interplay among the involved molecular regulators. Future studies will aim to elucidate the underlying regulatory mechanisms driving these phenomena. By highlighting the exact time- and quantity-dependent effects of the involved transcription factors, it might be possible to develop a deeper understanding of the influence of hypoxia on EMT.

Conflicts of Interest

The Authors declare that they have no competing interests.

Authors' Contributions

CT performed the experiments, analyzed the results and was a contributor to the manuscript. AVF supported conceiving the study, analyzed the results and was the primary author of the manuscript. CW conceived the study, analyzed the results and was a contributor to the manuscript. TEK and MS supported conceiving the study and analyzing the results. AS conceived the study, analyzed the results and was a contributor to the manuscript. SH interpreted the results and was a contributor to the manuscript. All Authors read and approved the final manuscript.

References

1 Bunn HF, Poyton RO: Oxygen sensing and molecular adaptation to hypoxia. Physiol Rev 76(3): 839-885, 1996. DOI: 10.1152/physrev.1996.76.3.839

2 Vaupel P, Mayer A, Höckel M: Tumor hypoxia and malignant progression. Methods Enzymol 381: 335-354, 2004. DOI: 10.1016/S0076-6879(04)81023-1

3 Becker A, Hänsgen G, Bloching M, Weigel C, Lautenschläger C, Dunst J: Oxygenation of squamous cell carcinoma of the head and neck: comparison of primary tumors, neck node metastases, and normal tissue. Int J Radiat Oncol Biol Phys 42(1): 35-41, 1998. DOI: 10.1016/s0360-3016(98)00182-5

4 Dachs GU, Tozer GM: Hypoxia modulated gene expression: Angiogenesis, metastasis and therapeutic exploitation. Eur J Cancer 36(13 Spec No): 1649-1660, 2000. DOI: 10.1016/s0959-8049(00)00159-3

5 Maynard MA, Evans AJ, Hosomi T, Hara S, Jewett MA, Ohh M: Human hif-3alpha4 is a dominant-negative regulator of hif-1 and is down-regulated in renal cell carcinoma. FASEB J 19(11): 1396-1406, 2005. DOI: 10.1096/fj.05-3788com

6 Huang LE, Arany Z, Livingston DM, Bunn HF: Activation of hypoxia-inducible transcription factor depends primarily upon redox-sensitive stabilization of its α subunit. J Biol Chem 271(50): 32253-32259, 1996. DOI: 10.1074/jbc.271.50.32253

7 Wenger RH: Cellular adaptation to hypoxia: O_2-sensing protein hydroxylases, hypoxia-inducible transcription factors, and O_2-regulated gene expression. FASEB J 16(10): 1151-1162, 2002. DOI: 10.1096/fj.01-0944rev

8 Tam SY, Wu VWC, Law HKW: Hypoxia-induced epithelial-mesenchymal transition in cancers: HIF-1α and beyond. Front Oncol 10: 486, 2020. DOI: 10.3389/fonc.2020.00486

9 Koh MY, Powis G: Passing the baton: the HIF switch. Trends Biochem Sci 37(9): 364-372, 2012. DOI: 10.1016/j.tibs.2012.06.004

10 Bartoszewski R, Moszyńska A, Serocki M, Cabaj A, Polten A, Ochocka R, Dell'Italia L, Bartoszewska S, Króliczewski J, Dąbrowski M, Collawn JF: Primary endothelial cell-specific regulation of hypoxia-inducible factor (HIF)-1 and HIF-2 and their target gene expression profiles during hypoxia. FASEB J 33(7): 7929-7941, 2019. DOI: 10.1096/fj.201802650RR

11 Scatozza F, D'Amore A, Fontanella RA, De Cesaris P, Marampon F, Padula F, Ziparo E, Riccioli A, Filippini A: Toll-Iike receptor-3 activation enhances malignant traits in human breast cancer cells through hypoxia-inducible factor-1α. Anticancer Res 40(10): 5379-5391, 2020. DOI: 10.21873/anticanres.14546

12 Zhong H, De Marzo AM, Laughner E, Lim M, Hilton DA, Zagzag D, Buechler P, Isaacs WB, Semenza GL, Simons JW: Overexpression of hypoxia-inducible factor 1alpha in common human cancers and their metastases. Cancer Res 59(22): 5830-5835, 1999.

13 Talks KL, Turley H, Gatter KC, Maxwell PH, Pugh CW, Ratcliffe PJ, Harris AL: The expression and distribution of the

hypoxia-inducible factors HIF-1alpha and HIF-2alpha in normal human tissues, cancers, and tumor-associated macrophages. Am J Pathol 157(2): 411-421, 2000. DOI: 10.1016/s0002-9440(10)64554-3

14 Semenza GL: Hypoxia, clonal selection, and the role of HIF-1 in tumor progression. Crit Rev Biochem Mol Biol 35(2): 71-103, 2000. DOI: 10.1080/10409230091169186

15 Patel NR, Jain L, Mahajan AM, Hiray PV, Shinde SS, Patel PA: An immunohistochemical study of HIF-1 alpha in oral epithelial dysplasia and oral squamous cell carcinoma. Indian J Otolaryngol Head Neck Surg 71(4): 435-441, 2019. DOI: 10.1007/s12070-019-01597-y

16 Hayashi Y, Yokota A, Harada H, Huang G: Hypoxia/pseudohypoxia-mediated activation of hypoxia-inducible factor-1α in cancer. Cancer Sci 110(5): 1510-1517, 2019. DOI: 10.1111/cas.13990

17 Horsman MR, Mortensen LS, Petersen JB, Busk M, Overgaard J: Imaging hypoxia to improve radiotherapy outcome. Nat Rev Clin Oncol 9(12): 674-687, 2012. DOI: 10.1038/nrclinonc.2012.171

18 Iommarini L, Porcelli AM, Gasparre G, Kurelac I: Non-canonical mechanisms regulating hypoxia-inducible factor 1 alpha in cancer. Front Oncol 7: 286, 2017. DOI: 10.3389/fonc.2017.00286

19 Semenza GL: HIF-1: mediator of physiological and pathophysiological responses to hypoxia. J Appl Physiol (1985) 88(4): 1474-1480, 2000. DOI: 10.1152/jappl.2000.88.4.1474

20 Grammatikaki S, Katifelis H, Stravodimos K, Bakolas E, Kavantzas N, Grigoriadou D, Gazouli M: The role of HIF1-related genes and non-coding RNAs expression in clear cell renal cell carcinoma. In Vivo 37(3): 1103-1110, 2023. DOI: 10.21873/invivo.13185

21 Miyata S, Ishii T, Kitanaka S: Reduction of HIF-1α/PD-L1 by catalytic topoisomerase inhibitor induces cell death through caspase activation in cancer cells under hypoxia. Anticancer Res 44(1): 49-59, 2024. DOI: 10.21873/anticanres.16787

22 Benita Y, Kikuchi H, Smith AD, Zhang MQ, Chung DC, Xavier RJ: An integrative genomics approach identifies Hypoxia Inducible Factor-1 (HIF-1)-target genes that form the core response to hypoxia. Nucleic Acids Res 37(14): 4587-4602, 2009. DOI: 10.1093/nar/gkp425

23 Beyer S, Kristensen MM, Jensen KS, Johansen JV, Staller P: The histone demethylases JMJD1A and JMJD2B are transcriptional targets of hypoxia-inducible factor HIF. J Biol Chem 283(52): 36542-36552, 2008. DOI: 10.1074/jbc.M804578200

24 Wellmann S, Bettkober M, Zelmer A, Seeger K, Faigle M, Eltzschig HK, Bührer C: Hypoxia upregulates the histone demethylase jmjd1a *via* hif-1. Biochem Biophys Res Commun 372(4): 892-897, 2008. DOI: 10.1016/j.bbrc.2008.05.150

25 Krieg AJ, Rankin EB, Chan D, Razorenova O, Fernandez S, Giaccia AJ: Regulation of the histone demethylase JMJD1A by hypoxia-inducible factor 1 alpha enhances hypoxic gene expression and tumor growth. Mol Cell Biol 30(1): 344-353, 2010. DOI: 10.1128/MCB.00444-09

26 Zhao M, Wang S, Zuo A, Zhang J, Wen W, Jiang W, Chen H, Liang D, Sun J, Wang M: HIF-1α/JMJD1A signaling regulates inflammation and oxidative stress following hyperglycemia and hypoxia-induced vascular cell injury. Cell Mol Biol Lett 26(1): 40, 2021. DOI: 10.1186/s11658-021-00283-8

27 Wilhelm C, Hackenberg S, Bregenzer M, Meyer T, Gehrke T, Kleinsasser N, Hagen R, Scherzad A: Effect of hypoxia on proliferation and the expression of the genes HIF-1α and JMJD1A in head and neck squamous cell carcinoma cell lines. Anticancer Res 41(1): 113-122, 2021. DOI: 10.21873/anticanres.14756

28 Wan W, Peng K, Li M, Qin L, Tong Z, Yan J, Shen B, Yu C: Histone demethylase JMJD1A promotes urinary bladder cancer progression by enhancing glycolysis through coactivation of hypoxia inducible factor 1α. Oncogene 36(27): 3868-3877, 2017. DOI: 10.1038/onc.2017.13

29 Tang DE, Dai Y, Xu SH: Histone demethylase JMJD1A promotes tumor progression *via* activating snail in prostate cancer. Mol Cancer Res 18(5): 698-708, 2020. DOI: 10.1158/1541-7786.MCR-19-0889

30 Macedo-Silva C, Miranda-Gonçalves V, Lameirinhas A, Lencart J, Pereira A, Lobo J, Guimarães R, Martins AT, Henrique R, Bravo I, Jerónimo C: JmjC-KDMs KDM3A and KDM6B modulate radioresistance under hypoxic conditions in esophageal squamous cell carcinoma. Cell Death Dis 11(12): 1068, 2020. DOI: 10.1038/s41419-020-03279-y

31 Dorna D, Paluszczak J: The Emerging significance of histone lysine demethylases as prognostic markers and therapeutic targets in head and neck cancers. Cells 11(6): 1023, 2022. DOI: 10.3390/cells11061023

32 Huang Y, Hong W, Wei X: The molecular mechanisms and therapeutic strategies of EMT in tumor progression and metastasis. J Hematol Oncol 15(1): 129, 2022. DOI: 10.1186/s13045-022-01347-8

33 Campbell K, Casanova J: A common framework for EMT and collective cell migration. Development 143(23): 4291-4300, 2016. DOI: 10.1242/dev.139071

34 Plygawko AT, Kan S, Campbell K: Epithelial-mesenchymal plasticity: emerging parallels between tissue morphogenesis and cancer metastasis. Philos Trans R Soc Lond B Biol Sci 375(1809): 20200087, 2020. DOI: 10.1098/rstb.2020.0087

35 Yang MH, Wu MZ, Chiou SH, Chen PM, Chang SY, Liu CJ, Teng SC, Wu KJ: Direct regulation of TWIST by HIF-1α promotes metastasis. Nat Cell Biol 10(3): 295-305, 2008. DOI: 10.1038/ncb1691

36 Zhang L, Huang G, Li X, Zhang Y, Jiang Y, Shen J, Liu J, Wang Q, Zhu J, Feng X, Dong J, Qian C: Hypoxia induces epithelial-mesenchymal transition *via* activation of SNAI1 by hypoxia-inducible factor -1α in hepatocellular carcinoma. BMC Cancer 13: 108, 2013. DOI: 10.1186/1471-2407-13-108

37 Liu KH, Tsai YT, Chin SY, Lee WR, Chen YC, Shen SC: Hypoxia stimulates the epithelial–to–mesenchymal transition in lung cancer cells through accumulation of nuclear β-catenin. Anticancer Res 38(11): 6299-6308, 2018. DOI: 10.21873/anticanres.12986

38 Joseph JP, Harishankar MK, Pillai AA, Devi A: Hypoxia induced EMT: A review on the mechanism of tumor progression and metastasis in OSCC. Oral Oncol 80: 23-32, 2018. DOI: 10.1016/j.oraloncology.2018.03.004

39 Rangan SRS: A new human cell line (FaDu) from a hypopharyngeal carcinoma. Cancer 29(1): 117-121, 1972. DOI: 10.1002/1097-0142(197201)29:1<117::aid-cncr2820290119>3.0.co;2-r

40 Gioanni J, Fischel JL, Lambert JC, Demard F, Mazeau C, Zanghellini E, Ettore F, Formento P, Chauvel P, Lalanne CM, Courdi A: Two new human tumor cell lines derived from squamous cell carcinomas of the tongue: Establishment, characterization and response to cytotoxic treatment. Eur J

Cancer Clin Oncol 24(9): 1445-1455, 1988. DOI: 10.1016/0277-5379(88)90335-5

41 Livak KJ, Schmittgen TD: Analysis of relative gene expression data using real-time quantitative PCR and the 2−ΔΔCT method. Methods 25(4): 402-408, 2001. DOI: 10.1006/meth.2001.1262

42 Vordermark D, Katzer A, Baier K, Kraft P, Flentje M: Cell type-specific association of hypoxia-inducible factor-1 alpha (HIF-1 alpha) protein accumulation and radiobiologic tumor hypoxia. Int J Radiat Oncol Biol Phys 58(4): 1242-1250, 2004. DOI: 10.1016/j.ijrobp.2003.11.030

43 Guo X, Shi M, Sun L, Wang Y, Gui Y, Cai Z, Duan X: The expression of histone demethylase JMJD1A in renal cell carcinoma. Neoplasma 58(2): 153-157, 2011. DOI: 10.4149/neo_2011_02_153

44 Park SJ, Kim JG, Son TG, Yi JM, Kim ND, Yang K, Heo K: The histone demethylase JMJD1A regulates adrenomedullin-mediated cell proliferation in hepatocellular carcinoma under hypoxia. Biochem Biophys Res Commun 434(4): 722-727, 2013. DOI: 10.1016/j.bbrc.2013.03.091

45 Essid N, Chambard JC, Elgaaïed AB: Induction of epithelial-mesenchymal transition (EMT) and Gli1 expression in head and neck squamous cell carcinoma (HNSCC) spheroid cultures. Bosn J Basic Med Sci 18(4): 336-346, 2018. DOI: 10.17305/bjbms.2018.3243

46 Zhu G, Peng F, Gong W, She L, Wei M, Tan H, Chen C, Zhang D, Li G, Huang D, Zhang X, Liu Y: Hypoxia promotes migration/invasion and glycolysis in head and neck squamous cell carcinoma *via* an HIF-1α-MTDH loop. Oncol Rep 38(5): 2893-2900, 2017. DOI: 10.3892/or.2017.5949

47 Shan Y, Li X, You B, Shi S, Zhang Q, You Y: MicroRNA-338 inhibits migration and proliferation by targeting hypoxia-induced factor 1α in nasopharyngeal carcinoma. Oncol Rep 34(4): 1943-1952, 2015. DOI: 10.3892/or.2015.4195

48 Yang J, Zhang X, Zhang Y, Zhu D, Zhang L, Li Y, Zhu Y, Li D, Zhou J: HIF-2α promotes epithelial-mesenchymal transition through regulating Twist2 binding to the promoter of E-cadherin in pancreatic cancer. J Exp Clin Cancer Res 35: 26, 2016. DOI: 10.1186/s13046-016-0298-y

49 Pollard PJ, Loenarz C, Mole DR, McDonough MA, Gleadle JM, Schofield CJ, Ratcliffe PJ: Regulation of Jumonji-domain-containing histone demethylases by hypoxia-inducible factor (HIF)-1α. Biochem J 416(3): 387-394, 2008. DOI: 10.1042/BJ20081238

50 Tang C, Liu T, Wang K, Wang X, Xu S, He D, Zeng J: Transcriptional regulation of FoxM1 by HIF-1α mediates hypoxia-induced EMT in prostate cancer. Oncol Rep 42(4): 1307-1318, 2019. DOI: 10.3892/or.2019.7248

51 Zhang Y, Wang X, Zhang M, Zhang Z, Jiang L, Li L: Gdf15 promotes epithelial-to-mesenchymal transition in colorectal [corrected]. Artif Cells Nanomed Biotechnol 46(sup2): 652-658, 2018. DOI: 10.1080/21691401.2018.1466146

52 Lemieux E, Bergeron S, Durand V, Asselin C, Saucier C, Rivard N: Constitutively active MEK1 is sufficient to induce epithelial-to-mesenchymal transition in intestinal epithelial cells and to promote tumor invasion and metastasis. Int J Cancer 125(7): 1575-1586, 2009. DOI: 10.1002/ijc.24485

53 Wang H, Wang Z, Li Y, Lu T, Hu G: Silencing snail reverses epithelial-mesenchymal transition and increases radiosensitivity in hypopharyngeal carcinoma. Onco Targets Ther 13: 497-511, 2020. DOI: 10.2147/OTT.S237410

Received May 21, 2024
Revised August 30, 2024
Accepted September 13, 2024